IUC UNIVERSITY PRESS iSTANBUL

REVIEW
Electrica 2026; 26: 1-13

Quad-Port Circularly Polarized Ring Slot Multiple-Input Multiple-Output Antenna for 5G UWB Wireless Communication Systems

Anjali Baliyan[1,2], Mohd Gulman Siddiqui[2], Karanjeet Singh Kharb[3], Ashish Singh[4]

[1]Department of Electronics and Communication Engineering, Maharaja Surajmal Institute of Technology, New Delhi, India
[2]Department of Physical Sciences, Banasthali Vidyapith, Jaipur, India
[3]Department of Electronics and Communication Engineering,Maharaja Surajmal Institute of Technology, New Delhi, India
[4]Department of Computer and Communication, NMAM Institute of Technology (NMAMIT), Nitte, Udupi, India

Cite this article as: A. Baliyan, M. G. Siddiqui, K. S. Kharb and A. Singh, "Quad-port circularly polarized ring slot multiple-input multiple-output antenna for 5G UWB wireless communication systems," *Electrica*, 26, 0258, 2026. doi: 10.5152/electrica.2026.25258.

ABSTRACT

A notable progress in antenna design, especially concerning multiple-input multiple-output (MIMO) antennas, is being driven by the emergence of 5G technology. One of the preliminary steps in constructing a multiple-input and multiple-output antenna involves choosing a suitable substrate material and thickness. The careful selection of dielectric substrate material and its thickness significantly influences the key characteristics such as physical dimensions, bandwidth, and radiation efficiency. This study presents the design and evaluation of a 4 × 4 circularly polarized multiple-input and multiple-output antenna tailored for 5G applications, with focus on evaluating four dielectric substrates, Flame Retardant 4, RT/Duroid5880, RT/Duroid6002, and Rogers RO3003. All antennas were modeled and investigated through full-wave simulations using ANSYS High-Frequency Structure Simulator, with a uniform substrate thickness of 0.8 mm. Based on simulated results, RT/Duroid 6002 was selected for fabrication. The fabricated antenna operates in the range of 15 GHz–45 GHz, and achieves a wide measured bandwidth of approximately 13.5 GHz in this operating range. Measurements were conducted using a vector network analyzer and an anechoic chamber. The envelope correlation coefficient was found to be 0.001, indicating excellent diversity performance along with diversity gain and total active reflection coefficient. The study provides valuable insights into the direct effects of dielectric substrate properties on an antenna's operation and guides substrate selection for the development of compact, wideband antenna arrays suitable for 5G mm-wave systems.

Index Terms—5G millimeter-wave communication, dielectric constant, diversity gain (DG), MIMO antenna systems, total active reflection coefficient (TARC)

I. INTRODUCTION

The primary objective of the previous generation of wireless mobile networks was to enhance personal connectivity for voice communication, data access, and video services. On the other hand, 5G, which was created as part of the Third Generation Partnership Project, is causing a fresh wave of innovation by spreading into several industrial applications. 5G is poised to transform industries with its high frequency capabilities, expanded channel capacity, low latency, and smooth integration with technologies like network slicing, cloud computing, and artificial intelligence/machine learning [1-4]. High-frequency spectrum bands are being used more and more by future 5G wireless systems to satisfy the increasing need to support a large number of users and applications. Communication solutions that can offer high-speed data rates with consistent quality are needed for the present and future 5G networks. Multiple-input and multiple-output (MIMO), a cutting-edge over-the-air communication technology, is essential to providing dependable, high-quality, and fast communications.

A significant breakthrough in wireless communication, MIMO antenna technology was first introduced to the world in the 1990s to overcome the limitations in data rates associated with old single-input single-output antennas [5-6]. The design of MIMO antenna systems involves the integration of multi-element antennas at both the transmitting and receiving ends, enabling

Corresponding author:
Anjali Baliyan

E-mail:
anjalibaliyan@msit.in

Received: August 22, 2025
Revision Requested: September 22, 2025
Last Revision Received: September 30, 2025
Accepted: October 7, 2025
Publication Date: January 26, 2026

DOI: 10.5152/electrica.2026.25258

Content of this journal is licensed under a Creative Commons Attribution-NonCommercial 4.0 International License.

a proportional increase in data rates with the number of antenna elements used [7]. The MIMO technology is widely utilized in modern over-the-air communication to enhance channel capacity, mitigate the effects of multipath propagation, and achieve higher data rates [8]. In recent years, the microstrip patch antennas have garnered widespread attention due to their compact dimensions and fabrication simplicity, and compatibility with integrated circuits, making them suitable for MIMO applications and a viable alternative to conventional antenna structures. In such a system, a significant problem can arise due to polarization mismatch losses. This problem can be overcome by using a circularly polarized antenna, as it eliminates the need to align the transmitting and receiving antennas [9]. Circularly polarized antennas are an excellent choice for providing stable communication due to their ability to provide controlled polarization mismatching and are resilient to multipath interference between the transmitting and the receiving antenna [10]. Along with these advantages, high-gain circularly polarized antenna arrays are employed to expand 5G wireless systems' coverage [11].

A key factor influencing the performance of circularly polarized MIMO antennas is the choice of dielectric substrate, which directly impacts parameters such as bandwidth, radiation efficiency, and impedance matching. Consequently, researchers have investigated various substrate materials to determine their suitability for high-frequency applications. In this study, a comparative analysis of four commonly employed dielectric substrates: flame retardant 4 (FR4) Glass Epoxy, Rogers RO3003, RT/Duroid 5880, and RT/Duroid 6002 is presented. All antennas are designed with a uniform thickness of 0.8 mm. The substrate thickness of all antenna designs is intentionally kept the same to exclude the effect of variation in substrates' height on the antenna's performance, as substrate thickness strongly affects antenna performance.

The analysis focuses on key performance parameters, including bandwidth, gain, voltage standing wave ratio (VSWR), envelope correlation coefficient (ECC), diversity gain (DG), total active reflection coefficient (TARC), and return loss [12]. Given the stringent requirements of 5G systems of high gain and wide bandwidth, compared to those of previous generations, the selection of an appropriate substrate material is essential for meeting next-generation communication standards. The material used to manufacture the antennas has a significant impact on these aspects. Therefore, it's critical to comprehend how various materials impact the performance of 5G antennas. In the previous six years, substantial research has been conducted on the design and development of 5G antennas, with a focus on different (broad) MIMO antenna types [13-17] and approaches to reduce isolation between antenna parts [18]. Researching different dual-band antenna topologies, notably rectangular slotted patch [19], substrate embedded waveguide [20], printed slot antenna [21], notched waveguide antenna [22], and planar inverted-F Antenna [23], which span the 28 GHz and 38 GHz bands, was suggested for 5G. Suggesting innovative 5G millimeter wave antennas that can be polarized in several ways, including dual dispersion [24] and circular polarization [25-27], and polarization re-configurability [28]. To the knowledge of the authors, no published work has comprehensively investigated the influence of various substrate innovations on 5G antennas' effectiveness.

II. DIELECTRIC SUBSTRATE CONSIDERATION FOR MIMO APPLICATIONS

A. Flame Retardant 4

Glass-reinforced epoxy laminate materials, including sheets and printed circuit boards, are categorized under the designation FR-4, or FR4. This composite material, known for its flame-proof and self-extinguishing properties, is constructed of woven fiberglass cloth embedded in epoxy resin binder. The FR4 is a widely used high-pressure thermoset laminate known for its high mechanical strength, low water absorption, and excellent electrical insulation capabilities, making it a reliable choice for a range of demanding electronic applications.

Its affordability and structural stability make it a practical choice for high-frequency applications, including 5G antenna systems, despite its relatively higher dielectric loss compared to advanced substrates.

B. RT/DUROID 6002

RT/Duroid 6002, developed by Rogers Corporation, is an advanced polytetrafluoroethylene (PTFE)-based laminate reinforced with ceramic fillers, engineered for microwave and radiofrequency (RF) applications. It features a low dielectric constant of 2.94 and excellent low-loss performance and consistent electrical behavior across wide temperature ranges, ensuring high signal integrity and efficiency in high-frequency environments with outstanding mechanical stability.

Its low moisture absorption and mechanical robustness make it well-suited for 5G antennas, radar systems, and satellite communications.

C. ROGERS RO3003

Rogers Corporation's RO3003 is a specialized laminate designed for advanced microwave and RF applications, offering reliable signal integrity across a broad frequency range with a low dielectric constant of 3.00. Composed of ceramic-filled PTFE, RO3003 ensures stable electrical performance under varying conditions by providing low moisture absorption, excellent thermal stability, and low dielectric loss.

These properties make it highly suitable for demanding environments such as satellite communications, high-frequency antennas, and radar systems, where precision, durability, and consistent performance in challenging environments are essential.

D. ROGERS RO3003

RT/Duroid 5880, produced by Rogers Corporation, is a premium high-performance microwave laminate renowned for its excellent behavior in high-frequency applications. It offers a low dielectric constant of 2.20 with an exceptionally low loss tangent, resulting from a PTFE matrix reinforced with glass microfibers. These properties ensure excellent signal integrity and high efficiency. The material also provides outstanding thermal stability, low moisture absorption, and reliable electrical consistency under harsh conditions. It is widely applied in antennas, radar systems, aerospace, defense, and advanced communication technology, where precision and stability are primary requirements.

The features of these different substrates are detailed below in Table I.

TABLE I. SUMMARY OF MATERIAL PROPERTIES FOR SELECTED SUBSTRATES

Properties	FR4	RO3003	RT/Duroid 5880	RT/Duroid 6002
Dielectric constant (ε_r)	4.4	3.0	2.2	2.94
Loss tangent (δ)	0.03	0.001	0.0009	0.0012
Cost	Low	Moderate	Expensive	Expensive
Temperature range	–40 to 130	–40 to 150	–55 to 200	–40 to 180
Applications	General-purpose electronics, consumer devices, automotive, and industrial systems	RF/microwave communication, satellite, radar, GPS, wireless links	Extreme RF/microwave applications, aerospace, military radar, satellite systems	Aerospace, defense, satellite communication, and high-performance antennas

III. ANTENNA CONFIGURATION

This work aims to design a microstrip patch MIMO antenna tailored and optimized for a range of 5G applications, with an emphasis on improved transmission and reception efficiency. The antenna is precisely modeled using ANSYS High-Frequency Structure Simulator, incorporating precisely defined dimensions to ensure accurate simulation and optimal performance. This program has incorporated slot cuts and improved the antenna's overall design to boost performance and efficiency. The resonance frequency of the antenna is set to be within 24 and 28 GHz, and its height is 0.8 mm. Fig. 1 illustrates the layout of the proposed antenna. The basic design consists of a circular patch surrounded by several circular rings, a micro-strip patch antenna, and a micro-strip feed line. These circular rings have two main functions: they enhance bandwidth and decrease return loss. The antenna has a full ground plane fitted on the rear side, made of 0.035 mm copper.

A. Single Element Antenna

As shown in the accompanying graphic, there are three separate steps in the antenna's design review process. The first stage involves building a circular patch antenna using the formula given in [29-30]. Circular rings are then added, each with a different radius depending on the substrate used, but all rings have the same thickness of 0.5 mm. The performance of the antenna is improved by this adjustment, especially about return loss and bandwidth. Two rectangular strips that are perpendicular to each other are added in the last step of the design. Wideband operation is made possible by this innovation, which significantly reduces the antenna's return loss. Fig. 1 shows the antenna's final configuration.

Variations in the dielectric constant of the different substrates used in the suggested antennas have an impact on the patch's size in the above picture, Fig. 1. Accordingly, Table II provides specific measurements for every patch.

The FR4, Rogers RO3003, RT/Duroid 5880, and RT/Duroid 6002 are the substrate materials used in the proposed study. These materials have relative permittivity of 4.4, 3.0, 2.2, and 2.94, respectively, and loss tangents of 0.02, 0.001, 0.0009, and 0.0012. The thickness of all substrates remains constant at 0.8 mm. Rings have been added to the circular patch antenna's design to increase its bandwidth. By altering the surface charge distribution, these rings enhance the current flowing through the circular patch, thereby widening the bandwidth. Essentially, the inclusion of these rings results in more capacitance, which disrupts the circular patch's reactance and significantly increases the antenna's impedance bandwidth. After the single element was used in the circular slots, it was then arranged in a 4×4 subarray structure.

B. 4×4 Multiple-Input Multiple-Output Antenna Design

The MIMO antenna is a symmetrical arrangement of four single elements that have been previously constructed on a shared substrate. The physical configuration and configuration of the antenna segments have a major impact on MIMO performance. For optimal performance, certain aspects, such as position, size, element distance, and overall shape, must be adjusted. Using techniques like separation or decoupling to reduce inter-element interference further can increase performance. The patches were placed to reduce interaction between the antenna elements with an across-the-edges spacing (D) of $\lambda/4$, where λ is the wavelength [31]. Expanding system capacity and increasing data transmission rates are the primary goals of these systems. Using a polarization diversity technique, a MIMO antenna system including either two or four elements was developed after a single antenna component was developed [32]. The evolution from a single antenna element to an optimized 4×4 MIMO array antenna configuration is displayed in Fig. 2.

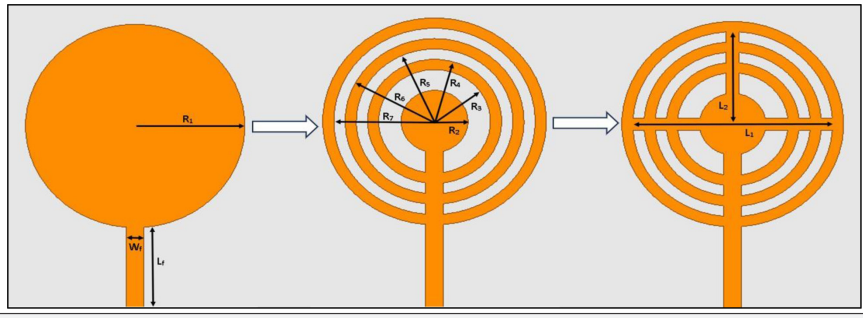

Fig. 1. Developmental stage of a single antenna patch.

TABLE II. OPTIMIZED ANTENNA ELEMENTS DESIGN PARAMETERS (MM)

Dimensions	FR4	Rogers RO3003	RT/Duroid 6002	RT/Duroid 5880
R_1	4.19	5.02	5	5.65
R_2	0.95	1.52	1.5	2.15
R_3	1.69	2.52	2.5	3.15
R_4	2.19	3.02	3	3.65
R_5	2.69	3.52	3.5	4.15
R_6	3.19	4.02	4	4.65
R_7	3.69	4.52	4.5	5.15
L_1	7.38	9.04	9	10.3
L_2	3.69	4.52	4.5	5.15
L_F	3.8	4.0	4.0	3.8
W_F	0.8	0.8	0.8	0.8

The final, optimized physical dimensions for the 4 × 4 MIMO antenna for improved performance across various substrates are presented in Table III.

C. Single Antenna Element

Fig. 3. shows the simulated findings for the reflection coefficient (S_{11}) with different substrates which are used in the designed 4 × 4 MIMO antenna. As illustrated in Fig. 3(a), the antenna exhibits S11 (return loss) values of −38.79 dB at 23.5 GHz, −28.31 dB at 31.8 GHz, −32.82 dB at 23 GHz, and −30.15 dB at 34.1 GHz for the proposed 4 × 4 MIMO antennas employing substrates RT/Duroid 6002, RT/Duroid 5880, Rogers RO 3003, and FR4. Each MIMO antenna's VSWR values remain below 2 at the assigned frequencies, which are 1.0232, 1.0799, 1.046, and 1.06 for RT/Duroid 6002, RT/Duroid 5880, Rogers RO 3003, and FR4, respectively, as visible in Fig. 3(b).

Several factors, like return loss, gain, directivity, and electrical field intensity, are used to assess a simple radiating patch antenna. When assessing a MIMO antenna, many important metrics need to be computed and analyzed, which are shown in Table IV.

Four substrates have been examined for the design of 4 × 4 MIMO antennas: FR4, Rogers RO 3003, RT/Duroid 6002, and RT/Duroid 5880. This study thoroughly examines a four-element, multiband, miniaturized MIMO antenna exhibiting exceptional bandwidth performance. The design is examined in detail following a thorough examination that spans the operating frequency range from 15 GHz to 45 GHz. The better results among the four simulated designs are obtained with RT Duroid 6002. Since loss tangent significantly affects bandwidth and radiation pattern, RT Duroid is an excellent dielectric substrate for MIMO antennas. Although it costs more compared to other substrate materials, its consistent high performance and dependability far outshine the cost, making it the most reliable option for sophisticated 5G applications. It is therefore proposed that RT Duroid be given precedence over the other three substrates under consideration. Based on these observations, RT Duroid 6002 was selected as the substrate for the fabricating a 4 × 4 MIMO antenna for 5G. Using this substrate enables observation of the antenna's practical performance and comparison between the simulated and experimentally measured performance metrics of the fabricated antenna. While fabricating the antenna, slight deviations in the materials or in fabrication processes can lead to discrepancies between the simulated results and the antenna's real-world performance. Variation in quality and thickness of copper (±5 µm) cladding can alter the surface current distribution and radio frequency losses, which can lead to a shift in resonant frequency by ~0.2–0.4 GHz and slightly affect the return loss. While surface finish, which can include production inconsistencies and poor surface finishing, may cause additional losses in antenna operation. Misalignment of 0.1 mm–0.2 mm in connectors can introduce parasitic inductance, resulting in impedance mismatch and variation in return loss by 5–10%. Variation in etching tolerance (±50 µm) and substrate inhomogeneity (±0.04 in dielectric constant, ±0.0012 in loss tangent for RT/Duroid 6002) can induce a shift in bandwidth and resonance by up to ~1GHz, minor degradation in polarization purity and reduction in efficiency of antenna by ~4-6%. To assure similar performance in both simulation and real-world, we orient the connectors accurately, ensure optimal isolation of the components, and rigorous compliance with the manufacturing protocols. The fabricated antenna for the chosen substrate is shown in Fig. 4.

TABLE III. OPTIMIZED MIMO ANTENNA DESIGN PARAMETERS (MM)

Dimensions (mm)	FR4	Rogers RO3003	RT/Duroid 6002	RD/Duroid 5880
L_S (Substrate length)	27.38	28.7	28.7	30
W_S (Substrate width)	27.38	30	30	30
P_D (Distance between patch)	4.5	3.5	3.6	3
A_L (Antenna length)	12.18	14.04	14	15.1

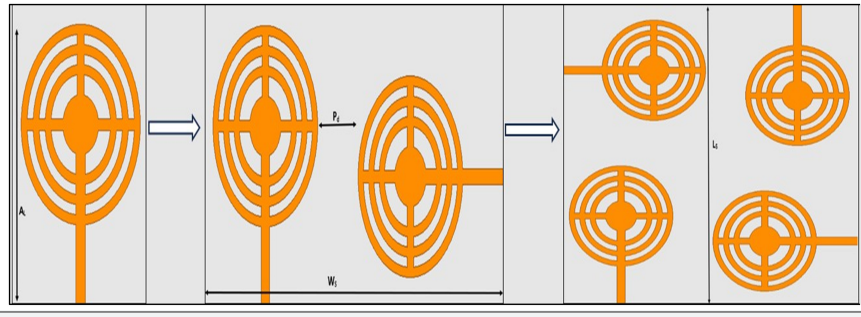

Fig. 2. Evolution of the proposed antenna structure: (a) Single element structure, (b) 2 × 2 MIMO antenna, (c) 4 × 4 MIMO configuration.

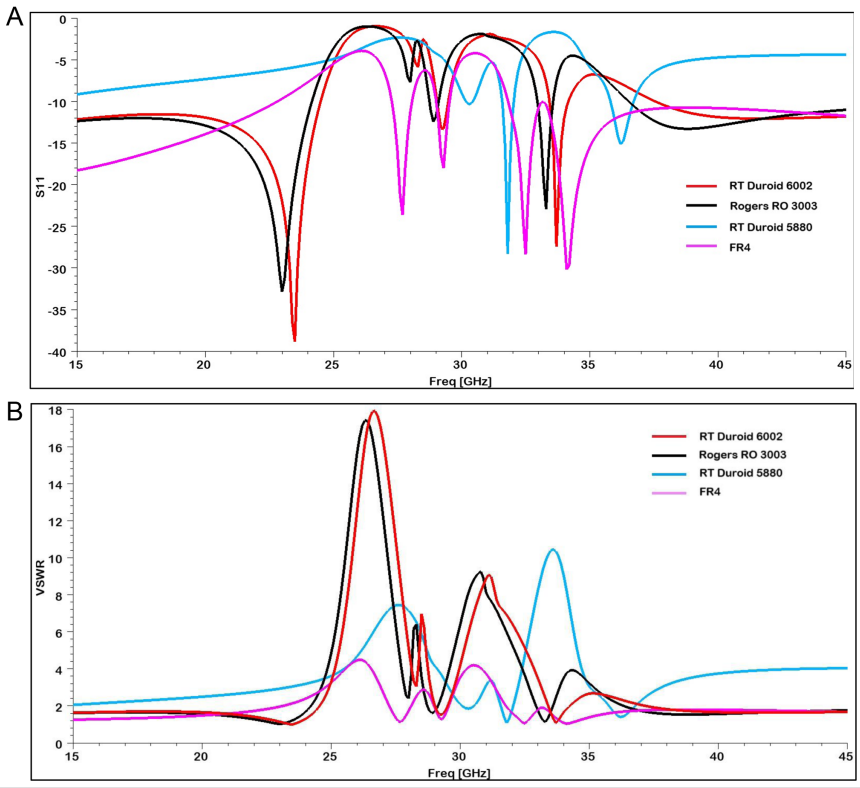

Fig. 3. Simulated analysis of 4 × 4 MIMO antenna (a) Return Loss, (b) VSWR.

IV. RESULTS

The validation process of the fabricated 4 × 4 MIMO antenna involves rigorous testing using a vector network analyzer (VNA) and an anechoic chamber to examine the far-field radiation characteristics using a standard reference horn antenna. Testing done in an anechoic chamber provides a reflection-free environment to accurately evaluate the antenna's radiation characteristics. A standard horn antenna captures signals from the MIMO antenna for evaluating radiation patterns. The evaluated outcomes using VNA and horn antenna, including VSWR, gain, isolation, TARC, ECC, radiation patterns, and return loss, are compared with the data obtained from simulation.

A. Scattering Parameters

In the analysis of MIMO antenna systems, S-parameters are crucial since they provide a comprehensive description of the entire system. Because each port represents a unique antenna element, S-parameters, as opposed to opportunity metrics, provide a more complete view of the antenna system by elucidating the relationships between them. By examining S-parameters, engineers can learn vital information about coupling, antenna interference, and isolation, all of which are essential for optimizing MIMO system performance. Through accurate characterization and iterative design enhancements, S-parameters significantly improve measurement and design flexibility. The reflection coefficient arcs for the comparison study for both simulated and measured results are displayed in Fig. 5, along with the proposed 4-port MIMO antenna's scattering characteristics. The symmetry of the antenna design explains the constant reflection coefficient (Sii) component in the results, where Sij equals Sji. Enabling all port responses makes the symmetrical response very evident. Furthermore, as illustrated in Fig. 6(a), the plot for simulated reflection coefficient shows exceptional performance by the antenna by remaining below −10 dB level throughout the operating frequency band, exhibiting an ultra-wide bandwidth of 18.4 GHz and minimum S11 value of −38.79 dB at 23.5 GHz, and in the case of the measured reflection coefficient for the fabricated antenna, the plot indicates excellent results in the operating range of 15 GHz to 45 GHz with S11 being below −10 dB for nearly 1/3 of the operating range, giving a total bandwidth of 13.5 GHz, with minimum value of −26.6 dB at 20 GHz. The same trend can be observed in the plot for VSWR for the simulated antenna and the fabricated antenna. In both cases, VSWR remains below the mark of 2 throughout the operating frequency band, as seen in Fig. 6(b). For the simulation, the minimum value of VSWR is observed to be 1.02 and 1.06 for the fabricated one.

TABLE IV. RESULT COMPARISON OF SIMULATED ANTENNAS

Antenna Parameter	FR4	Rogers RO3003	RT/ Duroid 6002	RT/ Duroid 5880
S11 (dB)	−30.1	−32.82	−38.79	−28.3
VSWR	1.06	1.046	1.023	1.079
Bandwidth (GHz)	16.3	17.8	18.4	1

B. Isolation

In a 4 × 4 MIMO antenna, mutual coupling between ports, represented by Sij, where i ≠ j, is a major concern, especially for the 5G frequency range applications, where high coupling can compromise performance. Minimizing it is vital due to manufacturing

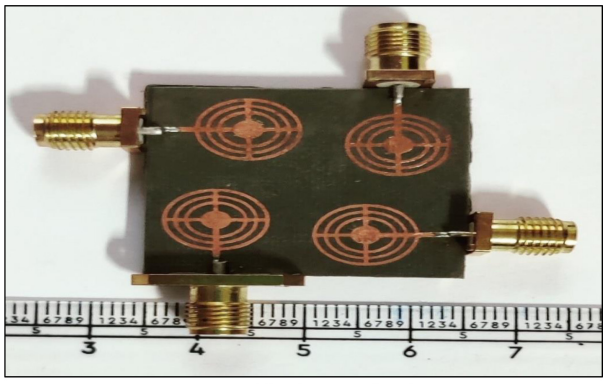

Fabricated antenna (a)front view

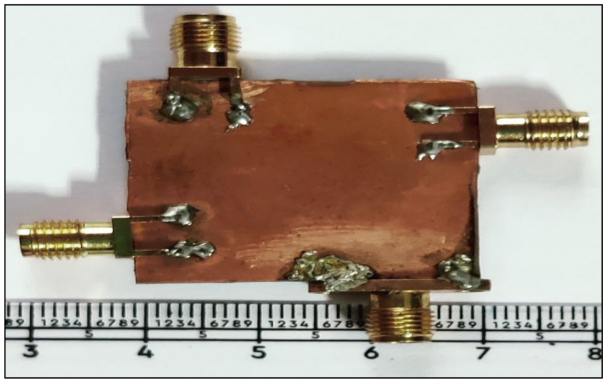

Fabricated antenna (b) back view

Fig. 4. Fabricated antenna (a) front and (b) back view.

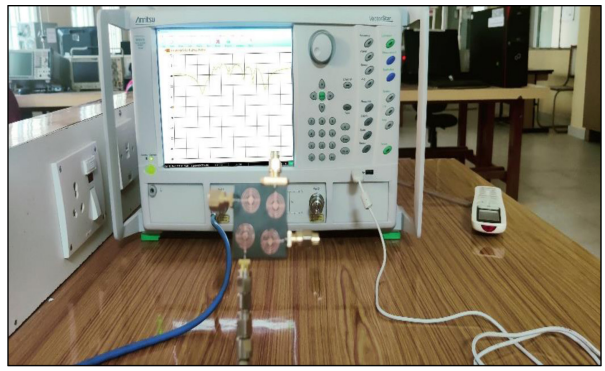

Experimental setup of fabricated antenna (a) VNA setup

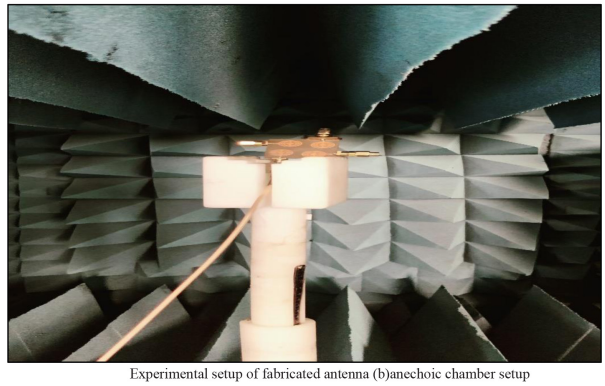

Experimental setup of fabricated antenna (b)anechoic chamber setup

Fig. 5. Experimental setup of fabricated antenna (a) VNA setup, (b) anechoic chamber setup.

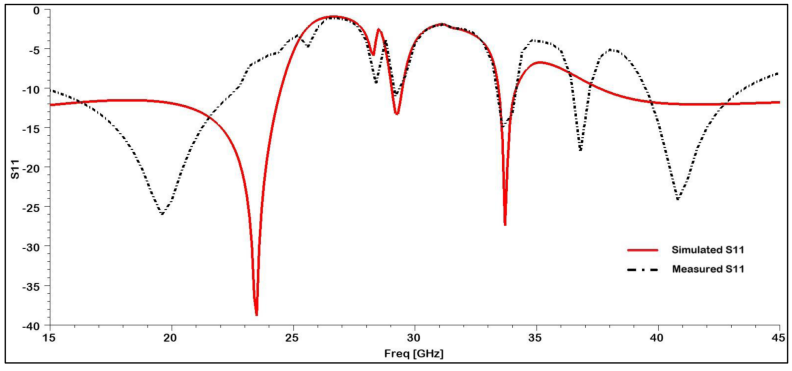

Simulated and Measured (a) Return loss S11

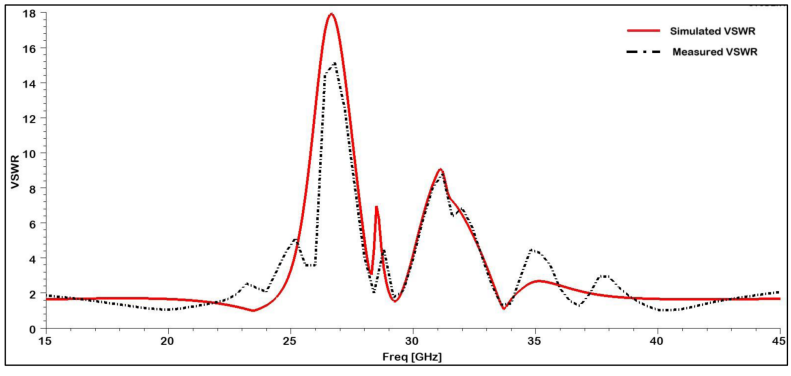

Simulated and Measured (b) VSWR

Fig. 6. Simulated and Measured (a) Return loss S_{11} and (b) VSWR.

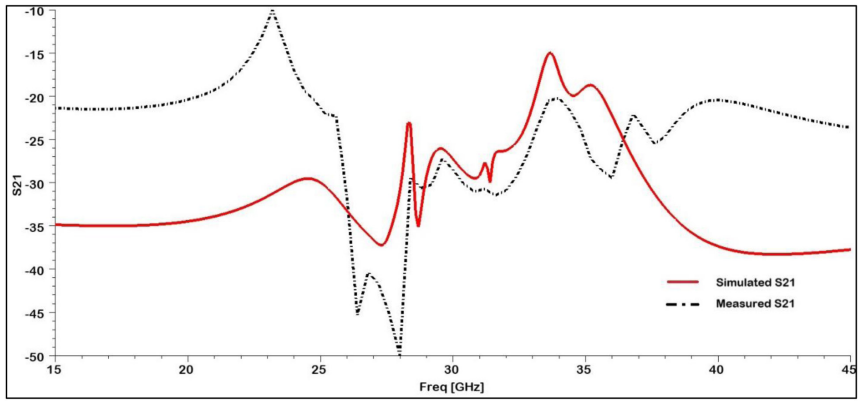

Fig. 7. Simulated and measured isolation of the proposed antenna.

precision and frequency scaling challenges. To guarantee that the antenna ports operate independently, this isolation must stay below −20 dB. The design successfully achieves this criterion, as the mutual coupling value, S12, consistently remains below −20dB across the entire operating frequency range for both simulated and measured antenna designs, with a minimum S21 value reaching −39dB for simulated and −49.9 dB for the measured one, as depicted in Fig. 7. This superior isolation is a direct result of a symmetrical arrangement of the antenna elements, inter-element spacing, and slot dimensions refined through precise development and optimization.

A more thorough evaluation of the isolation characteristics of the proposed MIMO antenna is conducted by examining the coupling behavior between diagonal and adjacent ports. The S-parameter plots are shown in Fig. 8, where diagonal port coupling is indicated by S_{13} and S_{24}, while S_{14} and S_{34} represent the adjacent port coupling.

The adjacent coupling is slightly higher than the diagonal coupling, as the ports are physically closer together. On the other hand, all coupling levels stay below −20 dB across the working bandwidth, indicating excellent isolation performance. The low coupling is the result of the combination of design elements. While the feed placement

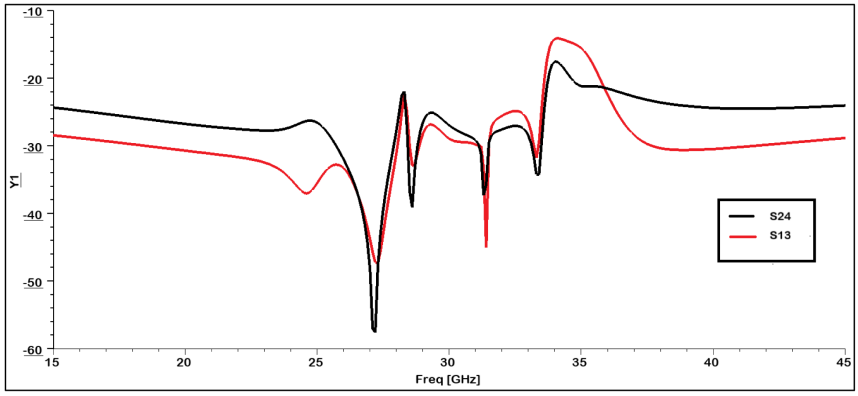

Isolation Performance of proposed antenna, (a) Diagonal Port Coupling

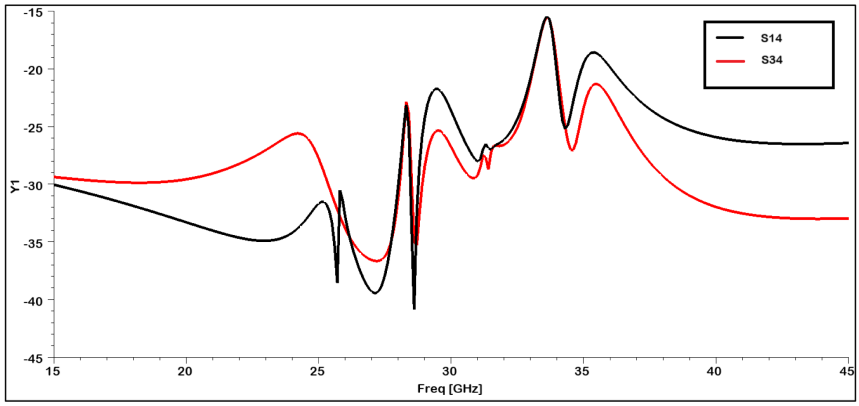

Isolation Performance of proposed antenna (b) Adjacent Port Coupling

Fig. 8. Isolation performance of proposed antenna, (a) diagonal port coupling and (b) sdjacent port coupling.

ensures destructive interference of coupled fields, the slot-ring geometry redistributes the surface currents to minimize unwanted interactions. Additionally, the antenna's structural symmetry further balances the fields, ensuring effective suppression of both diagonal and adjacent coupling.

C. Current Distribution

The surface current distribution in antenna engineering is the spatial pattern of induced electric currents that flow on an antenna surface when it is triggered by a radiofrequency signal. These currents are produced as a result of the applied electromagnetic field and the antenna's conducting surface. Electric fields are transformed into tangential surface currents as they cannot be sustained inside the antenna and act as the primary source of radiation. The current distributions with and without the Decoupling Structure (DS) are examined to better understand how this structure affects isolation levels. The DS's application efficiently concentrates surface currents on the activated antenna element while reducing interference with nearby antenna elements, as shown in Fig. 9. Surface current distribution in the proposed MIMO antenna at three different frequencies, which are 20 GHz, 28 GHz, and 38 GHz are presented.

D. Envelope Correlation Coefficient

The ECC in an antenna array arrangement measures the correlation between the signals' envelopes received from various antenna elements. An ECC value around 1 indicates strong coupling between the received signals, hence limiting the potential spatial DG that may be obtained with many antennas. The antennas' ability to enhance spatial variety through independent signal reception is demonstrated by a low ECC value [33]. The ECC is affected by the correlation coefficients and the magnitude of signal power being captured by the antenna sections. An ECC value below 0.5 is required for the best gearbox performance. Calculating the ECC reaction can be done using (1).

$$ECC = \frac{\left|S_{ii}^{*}S_{ij} + S_{ji}^{*}S_{jj}\right|^{2}}{\left(1-\left(\left|S_{ii}\right|^{2}+\left|S_{ji}\right|^{2}\right)\right)\left(1-\left(\left|S_{jj}\right|^{2}+\left|S_{ij}\right|^{2}\right)\right)} \quad (1)$$

Here, s_{ii} and s_{jj} stand for reflection coefficients, and S*ji* and S*ij* for transmission coefficients. Due to the presence of the complex conjugate representation (*), the dependability of the ECC accuracy when purely derived from the scattering parameters is subject to scrutiny. The far-field technique is therefore used to determine the ECC value [34].

Table V shows the ECC matrix of the fabricated 4 × 4 circularly polarized MIMO antenna, where all ECC values are found to be <0.5, confirming excellent diversity performance, low correlation, and validating the antenna's suitability for high-capacity 5G MIMO applications.

Fig. 10 depicts simulated and measured ECC values for the proposed 4 × 4 MIMO. Throughout the whole operating band, the ECC stays incredibly low, averaging 0.0001 (simulated) and 0.002 (measured). These results meet the ECC < 0.5 criteria for realistic MIMO systems, confirming outstanding diversity performance and negligible correlation between parts.

E. Diversity Gain

Utilising the spatial characteristics of the wireless channel, MIMO systems offer superior performance in comparison to single-antenna systems. Diversity gain, which uses an array of antennas

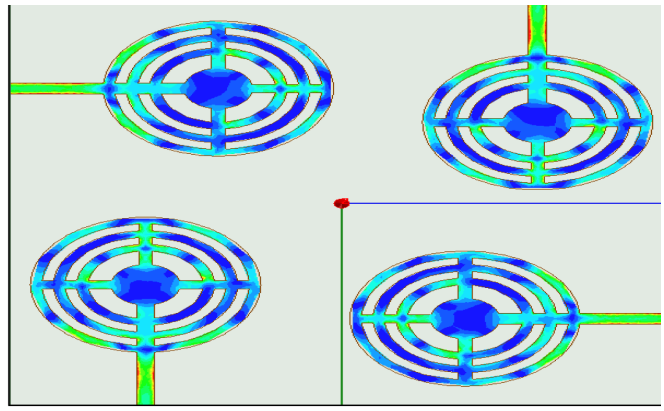

Surface Current Distribution of the proposed antenna at different frequencies, (a) at 20 GHz

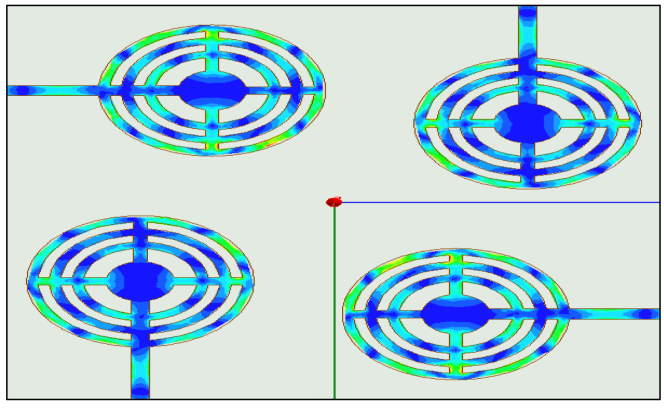

Surface Current Distribution of the proposed antenna at different frequencies (b) at 28 GHz

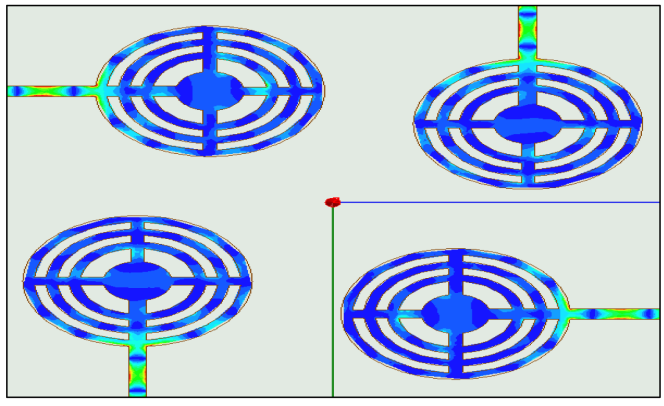

Surface Current Distribution of the proposed antenna at different frequencies (c) at 38 GHz

Fig. 9. Surface current distribution of the proposed antenna at different frequencies, (a) at 20 GHz, (b) at 28 GHz, and (c) at 38 GHz.

configured at the transmitting and receiving sides of the communication channel, significantly improves the signal fidelity of both the transmission and reception paths. The MIMO systems allow several signals in the same frequency band to be sent and received simultaneously by using multiple antennas. Environments with a range of channel conditions and more antennas generally have higher DG. The potential for diversity is diminished by tightly correlated channels, whereas uncorrelated channels enhance variety gain. Precoding, beamforming, and space-time coding are examples of advanced MIMO techniques that further increase the advantages of DG. To improve coverage, capacity, and reliability of wireless communication systems, the resulting MIMO DG is essential. When

Table V. ECC Matrix of Fabricated 4 × 4 MIMO Antenna

Port Pair	ECC value
ECC12	0.005832
ECC13	0.010858
ECC14	0.008041
ECC23	0.011044
ECC24	0.029671
ECC34	0.005936

assessing DG, the quantity of antennas, the properties of the channel, and their interrelationships must all be considered [35]. To compute DG, use (2) [36].

$$DG = 10\sqrt{1-|ECC|^2} \quad (2)$$

Fig. 11 shows the DG derived from the MIMO configuration's scattering properties. Within the designated ultra-wideband range, the DG remains above 9.9 dB for measured and near 10 dB for simulations, indicating the antennas' capacity to successfully reduce multipath fading and enable dependable wireless communication in wideband 5G scenarios.

F. Total Active Reflection Coefficient

The MIMO antenna systems must be designed and evaluated using TARC. The return loss experienced at the input of the antenna system by the transmitter is measured, accounting for active components such as amplifiers and matching networks. The greater the TARC number, the lower the performance is, since it signifies that part of the transmitted power is reflected to the transmitter. This reflected power may lead to issues like standing waves, an increase in interference, and decreased antenna efficiency. Therefore, TARC must be minimized while developing networks for wireless communication. This reduction is typically achieved by ensuring that the impedance of the antenna is equal to the transmission line and the transmitter, often by implementing network-based impedance matching techniques. A key consideration in assessing the proposed design is TARC, which is the proportion of input power radiated as useful energy, as stated in (3) [37]. The TARC values demonstrate the effectiveness of the presented MIMO antenna in isolating ports and optimizing output power, since they consistently fall below –4 dB across all frequency bands examined [38].

$$TARC = \sqrt{\frac{\left(\left(\left|S_{ii} + S_{ij}e^{j\theta}\right|^2\right) + \left(\left|S_{ji} + S_{jj}e^{j\theta}\right|^2\right)\right)}{2}} \quad (3)$$

θ represents the input phase angle.

Type the Paragraph Text

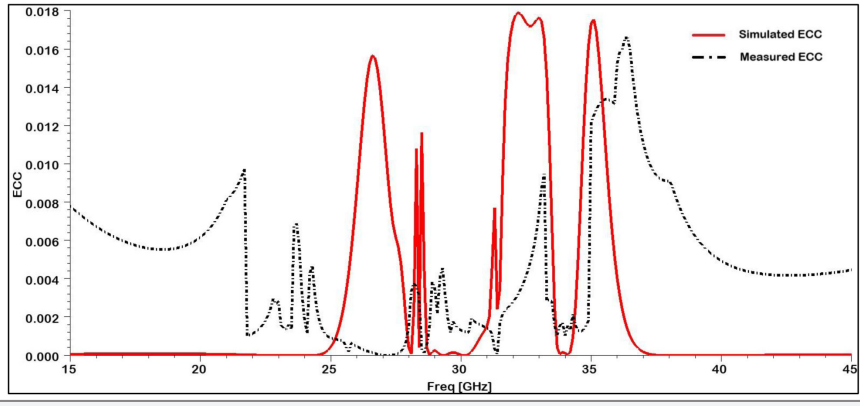

Fig. 10. Simulated and measured ECC.

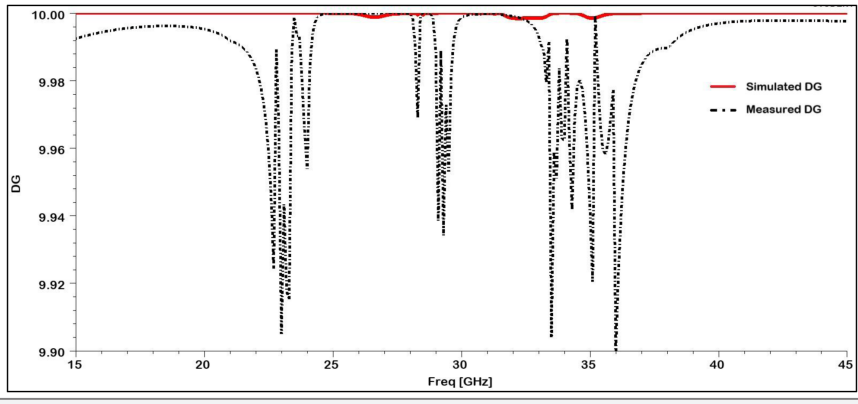

Fig. 11. Simulated and measured directive gain.

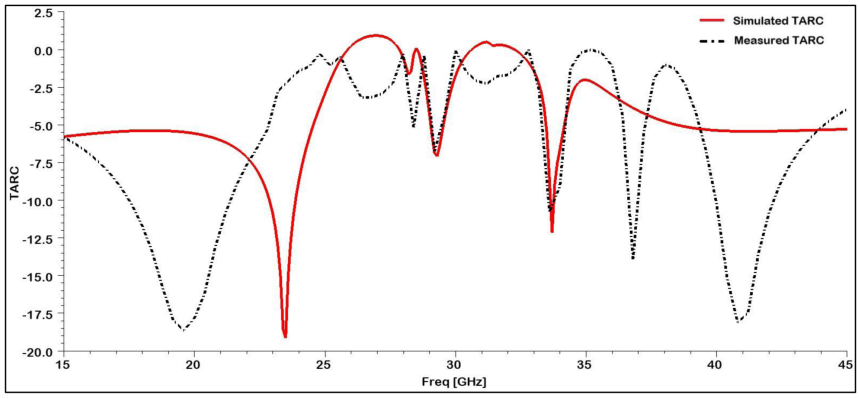

Fig. 12. Simulated and measured total active reflection coefficient (TARC).

TABLE VI. SUMMARY OF SIMULATED AND MEASURED PERFORMANCE PARAMETERS OF THE PRESENTED ANTENNA

Parameters	Simulated	Measured
Bandwidth (GHz)	18.5	13.5
ECC	0.0001	0.001
TARC (dB)	−19.1	−18.3
DG (dB)	~10	>9.9
Isolation (dB)	−38	−49
Peak gain (dB)	5.97	13.68

Fig. 12 plots the TARC values that were measured and simulated. In all scenarios, the TARC continuously drops below −4 dB throughout the band, suggesting minimal reflected power and effective port isolation. Furthermore, the consistency between the measured (−18.3 dB) and simulated (−19.1 dB) TARC values confirms that the suggested structure is successful in achieving high efficiency for MIMO operation.

The observed results closely match the simulated performance of the proposed antenna, as shown in Table VI, which summarizes the comparison of key parameters like bandwidth, ECC, TARC, diversity gain, isolation, and peak gain.

V. DISCUSSION

The fabricated MIMO antenna is capable of operations over multiple resonant frequency bands. A multi-band antenna operates over multiple frequency ranges, allowing it to support various communication standards or technologies within a single system. This enhances the antenna's adaptability and reduces the need for multiple dedicated antennas to cover different frequency bands. The antenna system exhibits low ECC values in both computational and measured findings, which can be attributed to minimal coupling and substantial

TABLE VII. COMPARATIVE ANALYSIS OF PROPOSED WORK WITH EXISTING MIMO ANTENNA DESIGNS

Ref No.	No. of Ports	Operating Frequency	Bandwidth	Peak Gain	Isolation	ECC	TARC	DG	Size	Technique Used
[39]	4	3.69–6.53	2.85	5.9	<−25	0.002	–	–	44 × 44	DGS, slotted patch, parasitic strips
[40]	2	5.2–5.7 11.8–17.3	6	5.5	<−20	0.004	−10	>9.9	30 × 30	DGS, slotted patch, parasitic element
[41]	6	26–29.5	3.5	5.6	<−20	0.04	–	>9.5	75 × 100	DGS, slotted patch
[42]	4	26–32.7	6.7	11	<−20	0.002	–	>9.9	4.7 × 2.9	DGS, modified patch
[43]	2	3.3–7.8 8.0–12.0	8.5	4	<−20	0.06	−9	>9.8	32 × 20	DGS, slotted patch
[44]	4	24.1–27.18	3.08	3	−16	0.1	−15	>9	20 × 24	Slotted patch
[43]	4	2108–29.1	7.30	5.76	<−18	0.004	<−2	–	31.9 × 37.6	DGS, slotted patch
[45]	2	34.1–39.7	5.6	6.7	<−20	0.003	−20	>9.9	6 × 17.37	DGS, modified patch
[46]	4	3.36–3.7 4.9–5.6	1.04	4	<−18	0.001	–	>8.8	26 × 26	DGS, slotted patch
[47]	4	28/38	1.2	8.13	<−20	0.0030	–	>9.9	4.95 × 5.8	DGS slotted patch
This Work	4	15–23.5, 39–44	13.5	13.7	<−20	0.001	−18.3	>9.9	28.7 × 30	Slotted patch

spatial diversity. Excellent impedance matching is demonstrated by the antenna, as indicated by the return loss consistently remaining below the −10 dB mark at the operating frequency range. The S21 results measured for the MIMO antenna also exhibit a similar trend to the simulated data, remaining below −20 dB across the operating frequency. While deviations are observed among simulated and measured results, even under worst-case conditions, isolation does not exceed the −18 dB mark. Excellent diversity performance is demonstrated by the 4 × 4 MIMO antenna, as evidenced by measured DG values continuously reaching 10 dB, ensuring effective mitigation of multipath fading, thereby supporting reliable and stable communication, especially in complex environments such as indoor settings and urban areas. A comparative analysis based on the core design and evaluation criteria is presented *in* Table VII, highlighting the superior radiation characteristics of the developed MIMO antenna in aspects of gain, bandwidth, and diversity performance.

VI. CONCLUSION

This paper outlines the architecture and evaluation of a 4 × 4 circularly polarized MIMO antenna system for 5G millimeter-wave applications employing four different dielectric substrates. The antenna incorporates a circular patch geometry to achieve high impedance bandwidth and strong circular polarization, making it suitable for 5G MIMO applications. It achieves an impressive bandwidth of 13.5 GHz, excellent isolation with components spaced over 25 dB apart, near omnidirectional radiation patterns, minimal ECC (~0.001), and high DG (>9.9 dB). These results align precisely with the intended design for MIMO antennas in mm-wave applications, and emphasize the critical role of substrate selection in achieving optimal performance. While the fabricated prototype confirmed the antenna's overall effectiveness, the measured results were inferior to the simulated predictions due to fabrication tolerances, misalignment during assembly, substrate inhomogeneity, and connector losses. These can be minimized through precise fabrication techniques and refined simulation models that account for real-world losses and assembly variations.

Although the slot-ring geometry is intended for 5G mm-Wave operation, it offers inherent scalability. Use of advanced low-loss substrates like LTCC (Low Temperature Co-fired Ceramic) and engineered metamaterials and minor changes to dimensions can enable it to operate in the sub-THz (100-300 GHz) band, a spectrum of increasingly important 6G technologies. The design can be scaled to larger MIMO arrays to meet the capacity and spatial diversity requirements of massive MIMO systems. Thus, the proposed MIMO antenna offers a reliable foundation for developing high-performance, versatile, and scalable architecture for future-generation wireless communication networks.

Data Availability Statement: The data that support the findings of this study are available on request from the corresponding author.

Peer-review: Externally peer-reviewed.

Author Contributions: Concept – A.B., K.S.; Design – A.B., K.S.; Supervision – M.G.S., Resources – M.G.S, A.S.; Materials – M.G.S., A.S.; Data Collection and/or Processing – A.B., M.G.S.; Analysis and/or Interpretation – A.B., M.G.S.; Literature Search – A.B., K.S.; Writing – A.B., K.S.; Critical Review – M.G.S., A.S.

Declaration of Interests: The authors have no conflicts of interest to declare.

Funding: The authors declared that this study has received no financial support.

REFERENCES

1. V. Kikan, and A. Kumar, "A detailed review of 5G MIMO and array antenna design evolution with performance enhancement for mmWave applications," *Wirel. Netw.*, vol. 31 pp. 2039–2090, 2024.
2. M. Series, "IMT Vision—Framework and overall objectives of the future development of IMT for 2020 and beyond," *Recommendation ITU*, vol. 2083, no. 0, pp. 1–21, 2015.
3. S. Kumar, A. S. Dixit, R. R. Malekar, H. D. Raut, and L. K. Shevada, "Fifth-generation antennas: A comprehensive review of design and performance enhancement techniques," *IEEE Access*, vol. 8, pp. 163568–163593, 2020. [CrossRef]
4. M. Agiwal, A. Roy, and N. Saxena, "Next generation 5G wireless networks: A comprehensive survey," *IEEE Commun. Surv. Tutor.*, vol. 18, no. 3, pp. 1617–1655, 2016. [CrossRef]
5. H. Yon, N. H. Abd Rahman, M. A. Aris, M. H. Jamaluddin, and H. Jumaat, "Parametric study on mutual coupling reduction for MIMO future 5G antennas," *J. Electr. Electron. Syst. Res. (JEESR)*, vol. 16, no. JUNE 2020, pp. 59–65, 2020. [CrossRef]
6. M. S. Sharawi, *Printed MIMO Antenna Engineering*. Artech House, 2014.
7. M. Nedil, "Coupling reduction between dipole antennas," *IEEE Antennas Propag. Mag.*, vol. 16, pp. 3–4, 2016.
8. H. Alsaif, "Extreme wide-band MIMO antenna system for fifth generation wireless systems," *Eng. Technol. Appl. Sci. Res.*, vol. 10, no. 2, pp. 5492–5495, 2020. [CrossRef]
9. E. Thakur, N. Jaglan, A. Gupta, and A. J. A. Al-Gburi, "Multi-band notched circular polarized MIMO antenna for ultra-wideband applications," *Prog. Electromagn. Res. M*, vol. 125, pp. 87–95, 2024. [CrossRef]
10. F. Taher et al., "Design and analysis of circular polarized two-port MIMO antennas with various antenna element orientations," *Micromachines*, vol. 14, no. 2, p. 380, 2023. [CrossRef]
11. H. Xu, P. Wei, S. Jiang, Z. Yu, J. Zhou, and C. Liu, "Wideband circularly polarized planar U-shaped antenna array for millimeter-wave applications," *IEEE Trans. Antennas Propag*, vol. 71, no. 8, pp. 6971–6976, 2023. [CrossRef]
12. A. Khan, and R. Nema, "Analysis of five different dielectric substrates on microstrip patch antennas," *Int. J. Comput. Appl.*, vol. 55, no. 14, pp. 40–47, 2012. [CrossRef]
13. B. Yang, Z. Yu, Y. Dong, J. Zhou, and W. Hong, "Compact tapered slot antenna array for 5G millimeter-wave massive MIMO systems," *IEEE Trans. Antennas Propag*, vol. 65, no. 12, pp. 6721–6727, 2017. [CrossRef]
14. M. M. M. Ali, and A. R. Sebak, "Design of a compact millimeter wave massive MIMO dual-band (28/38 GHz) antenna array for future 5G communication systems," In 2016, 17th International Symposium on Antenna Technology and Applied Electromagnetics (ANTEM). New York: IEEE, 2016, pp. 1–2. [CrossRef]
15. N. O. Parchin, M. Shen, and G. F. Pedersen, "End-fire phased array 5G antenna design using leaf-shaped bow-tie elements for 28/38 GHz MIMO applications," In IEEE International Conference on Ubiquitous Wireless Broadband (ICUWB). New York: IEEE, 2016, pp. 1–4. [CrossRef]
16. N. Ojaroudiparchin, M. Shen, and G. Fr, "Multi-layer 5G mobile phone antenna for multi-user MIMO communications" In 2015, 23rd Telecommunications Forum Telfor (TELFOR). New York: IEEE, 2015, pp. 559–562.
17. O. M. Haraz, M. Ashraf, and S. Alshebeili, "Single-band PIFA MIMO antenna system design for future 5G wireless communication applications," In 11th International Conference on Wireless and Mobile Computing, Networking, and Communications (WiMob). New York: IEEE, 2015, pp. 608–612. [CrossRef]
18. D. T. T. Tu, N. G. Thang, N. T. Ngoc, N. T. B. Phuong, and V. Van Yem, "28/38 GHz dual-band MIMO antenna with low mutual coupling using novel round patch EBG cells for 5G applications," In 2017 International Conference on Advanced Technologies for Communications (ATC). New York: IEEE, 2017, pp. 64–69.
19. M. K. M. Amin, M. F. Mansor, N. Misran, and M. T. Islam, "28/38GHz dual-band slotted patch antenna with proximity-coupled feed for 5G communication," In International Symposium on Antennas and Propagation (ISAP). New York: IEEE, 2017, pp. 1–2. [CrossRef]
20. N. Ashraf, O. Haraz, M. A. Ashraf, and S. Alshebeili, "28/38-GHz dual-band millimeter-wave SIW array antenna with EBG structures for 5G applications" In The 2015 international conference on information and communication technology research (ICTRC). New York: IEEE, 2015, pp. 5–8. [CrossRef]
21. O. M. Haraz, M. M. M. Ali, S. Alshebeili, and A. R. Sebak, "Design of a 28/38 GHz dual-band printed slot antenna for the future 5G mobile

communication networks," In IEEE International Symposium on Antennas and Propagation & USNC/URSI National Radio Science Meeting. New York: IEEE, 2015, pp. 1532–1533. [CrossRef]
22. I. F. da Costa, S. A. Cerqueira, and D. H. Spadoti, "Dual-band slotted waveguide antenna array for adaptive mm-wave 5G networks," In 2017 11th European conference on antennas and propagation (EUCAP). New York: IEEE, 2017, pp. 1322–1325.
23. W. Ahmad, and W. T. Khan, "Small form factor dual band (28/38 GHz) PIFA antenna for 5G applications," In IEEE MTT-S International Conference on Microwaves for Intelligent Mobility (ICMIM). New York: IEEE, 2017, pp. 21–24. [CrossRef]
24. J. K. Du et al., "Dual-polarized patch array antenna package for 5G communication systems," In 11th European Conference on Antennas and Propagation (EUCAP). New York: IEEE, 2017, pp. 3493–3496. [CrossRef]
25. H. Aliakbari, A. Abdipour, R. Mirzavand, A. Costanzo, and P. Mousavi, "A single-feed dual-band circularly polarized millimeter-wave antenna for 5G communication" In The 2016 10th European conference on antennas and propagation (EuCAP). New York: IEEE, 2016, pp. 1–5. [CrossRef]
26. M. Nosrati, and N. Tavassolian, "A single-feed dual-band, linearly/circularly polarized cross-slot millimeter-wave antenna for future 5G networks," In IEEE International Symposium on Antennas and Propagation & USNC/URSI National Radio Science Meeting. New York: IEEE, 2017, pp. 2467–2468. [CrossRef]
27. W. Lin, R. W. Ziolkowski, and T. C. Baum, "28 GHz compact omnidirectional circularly polarized antenna for device-to-device communications in the future 5G systems," *IEEE Trans. Antennas Propag.*, vol. 65, no. 12, pp. 6904–6914, 2017. [CrossRef]
28. E. A. Al Abbas, A. T. Mobashsher, and A. Abbosh, "Polarization reconfigurable antenna for 5G cellular networks operating at millimeter waves," In IEEE Asia Pacific Microwave Conference (APMC). New York: IEEE, 2017, pp. 772–774. [CrossRef]
29. S. Ghoneim, "Design and characterization of compact broadband antenna and its MIMO configuration for 28 GHz 5G applications," *Electronics (Switzerland)*, vol. 11, no. 4, Art. no. 523, 2022.
30. N. Hussain et al., "A compact flexible frequency reconfigurable antenna for heterogeneous applications," *IEEE Access*, vol. 8, pp. 173298–173307, 2020. [CrossRef]
31. Y. Amraoui, I. Halkhams, R. E. El Alami, M. O. Jamil, and H. Qjidaa, "High-gain MIMO antenna with multiband characterization for terahertz applications," *Sci. Afr.*, vol. 26, e02380, 2024. [CrossRef]
32. W. T. Sethi, S. H. Kiani, M. E. Munir, D. A. Sehrai, D. Awan, and D. Awan, "Pattern diversity-based four-element dual-band MIMO patch antenna for 5G mmWave communication networks," *J. Infrared Milli. Terahz Waves*, vol. 45, no. 5–6, pp. 521–537, 2024. [CrossRef]
33. K. Pandya et al., "Performance analysis of a quad-port UWB MIMO antenna system for Sub-6 GHz 5G, WLAN, and X Band communications," *Results Eng.*, vol. 22, 102318, 2024. [CrossRef]
34. A. Baz, D. Jansari, S. P. Lavadiya, and S. K. Patel, "Miniaturized and high-gain circularly slotted 4×4 MIMO antenna with diversity performance analysis for 5G/wi-fi/WLAN wireless communication applications," *Results Eng.*, vol. 20, 101505, 2023. [CrossRef]
35. A. Ahmad, D. Y. Choi, and S. Ullah, "A compact two-element MIMO antenna for 5G communication," *Sci. Rep.*, vol. 12, no. 1, p. 3608, 2022. [CrossRef]
36. D. M. John et al., "A compact flexible four-element dual-band antenna using a unique defective ground decoupling structure for sub-6 GHz wearable applications," *Results Eng.*, vol. 21, 101900, 2024. [CrossRef]
37. D. Srikar et al., "A novel integrated UWB sensing and 8-element MIMO communication cognitive radio antenna system," *Electronics*, vol. 12, no. 2, p. 330, 2023. [CrossRef]
38. H. Islam et al., "Compact circularly polarized 2 and 4-port multiple input, multiple output antennas with bandstop filter isolation technique," *Alex. Eng. J.*, vol. 66, pp. 357–376, 2023. [CrossRef]
39. P. Pradeep, J. S. Kottareddygari, and C. S. Paidimarry, "A compact 4x4 peace-shaped wideband MIMO antenna for Sub-6 GHz 5G wireless applications," *Int. J. Microw. Opt. Technol.*, vol. 17, no. 5, 2022.
40. A. Ali, M. E. Munir, M. M. Nasralla, M. A. Esmail, A. J. A. Al-Gburi, and F. A. Bhatti, "Design process of a compact tri-band MIMO antenna with wideband characteristics for sub-6 GHz, Ku-band, and millimeter-wave applications," *Ain Shams Eng. J.*, vol. 15, no. 3, 102579, 2024. [CrossRef]
41. S. Iffat Naqvi et al., "Integrated LTE and millimeter-wave 5G MIMO antenna system for 4G/5G wireless terminals," *Sensors (Basel)*, vol. 20, no. 14, p. 3926, 2020. [CrossRef]
42. A. Allah, H. Ahmad, M. Sohail, W. Zaman, M. Ismail, and M. Rahman, "A novel high gain array approach MIMO antenna operating at 28 GHz for 5G mm Wave applications," In 1st International Conference on Microwave, Antennas & Circuits (ICMAC). New York: IEEE, 2021, pp. 1–4. [CrossRef]
43. A. G. Alharbi, J. Kulkarni, A. Desai, C.-Y.-D. Sim, and A. Poddar, "A multi-slot two-antenna MIMO with high isolation for Sub-6 GHz 5G/IEEE802.11ac/ax/C-Band/X-band wireless and satellite applications," *Electronics*, vol. 11, no. 3, p. 473, 2022.[CrossRef]
44. A. Desai, C. D. Bui, J. Patel, T. Upadhyaya, G. Byun, and T. K. Nguyen, "Compact wideband four element optically transparent MIMO antenna for mm-wave 5G applications," *IEEE Access*, vol. 8, pp. 194206–194217, 2020. [CrossRef]
45. O. Elalaouy, M. E. Ghzaoui, and J. Foshi, "A high-isolated wideband two-port MIMO antenna for 5G millimeter-wave applications," *Results Eng.*, vol. 23, 102466, 2024. [CrossRef]
46. W. F. A. Mshwat et al., "Compact reconfigurable MIMO antenna for 5G and wi-fi applications," *IEEE Access*, vol. 12, pp. 110283–110298, 2024. [CrossRef]
47. R. R. Elsharkawy, K. F. A. Hussein, and A. E. Farahat, "Dual-band (28/38 GHz) compact MIMO antenna system for millimeter-wave applications," *J. Infrared Milli. Terahz Waves*, vol. 44, no. 11–12, pp. 1016–1037, 2023. [CrossRef]

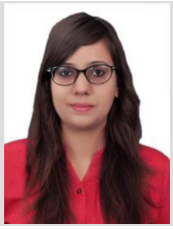

Anjali Baliyan Graduated in Electronics and Communication Engineering from Trident Group of Institutions, Ghaziabad, India in 2014. She received the MTech degree in Electronics and Communication Engineering from USICT, GGSIPU, Dwarka, New Delhi, India, in 2017. She is currently pursuing a Ph.D. in antennas and microwave domain from the Department of Electronics and Communication, Banasthali Vidyapith, Rajasthan. She is currently working as an Assistant Professor with the Department of Electronics and Communication Engineering, Maharaja Surajmal Institute of Technology, Delhi. She has published two papers at conferences. Her research areas include microstrip antennas, MIMO antennas for 5G.

Mohd Gulman Siddiqui Graduated in electronics and communication engineering from S.I.E.T., Allahabad, India, in 2011. He received the MTech. degree in electronics and communication from the Amity School of Engineering and Technology, Amity University, Noida, India, and the Ph.D. degree in antenna and microwave domain from the Department of Electronics and Communication, University of Allahabad, Allahabad, in 2019. He is currently working as an Assistant Professor with the Department of Physical Sciences, Banasthali Vidyapith, Rajasthan. He has published more than 30 research papers, including journals, conferences and book chapters. His research area includes microstrip antenna, wearable antenna, reconfigurable antenna for IOT and 5G, wireless communication, and soft-computing techniques.

Karanjeet Singh Kharb Graduated in Electronics and Communication Engineering from Maharaja Surajmal Institute of Technology, GGSIPU, Delhi, India in the year 2024. He has co-authored research papers in the field of antennas for 5G communication. His research interests include multiple-input multiple-output systems, millimetre-wave and terahertz communication, reconfigurable antenna technologies, and next-generation wireless communication technologies

Ashish Singh Graduated in Applied Electronics and Instrumentation from the Uttar Pradesh Technical University, India, in 2007. He completed his M.Tech. and D.Phil. degrees in Communication Technology from the Department of Electronics and Communication, University of Allahabad (A Central University) in 2009 and 2015, respectively. He has published more than 40 research papers in different national and international journals and conference proceedings. His areas of interest are Patch Antenna, Millimetre waves, Optical communication, Nano Antenna and Bio-medical Instrumentation. He worked as an Assistant Professor in Raghu Engineering College, Visakhapatnam. Presently, he is working at the same position in NMAM Institute of Technology, Nitte India.